

Influence of zinc acetate content on the photoelectrochemical performance of zinc oxide nanostructures fabricated by electrospinning technique

Nanomaterials and Nanotechnology Volume 6: I-7 © The Author(s) 2016 DOI: 10.1177/1847980416663679 nax.sagepub.com



Pierre G Ramos¹, Noé J Morales¹, Roberto J Candal^{2,3}, Mirabbos Hojamberdiev⁴, and Juan Rodriguez¹

Abstract

One-dimensional nanostructures have shown high photocatalytic efficiency due to their high surface area to volume ratio and charge transfer efficiency. In this work, we have studied the influence of zinc acetate content (zinc acetate to polyvinyl alcohol (PVA) mass ratio) on the photoelectrochemical performance of zinc oxide (ZnO) nanostructures. The nanostructures of ZnO were fabricated on fluorine-doped tin oxide glass substrate by electrospinning of aqueous solution containing different amounts of zinc acetate. The precursor nanofibers of zinc acetate/PVA were converted into polycrystalline ZnO nanostructures with hexagonal wurtzite crystal structure by calcination at 600°C for 3 h. It was found that by increasing the amount of zinc acetate, the diameter of the as-spun precursor fibers increased and their distribution became broader. The mean diameter of the ZnO nanoparticles forming the nanostructures ranged from 45 to 80 nm by increasing the amount of zinc acetate. The incident photon to current efficiency (IPCE) spectra of the ZnO nanostructures were measured in a three-electrode cell, using a platinum wire as a counterelectrode and silver/silver chloride as a reference electrode. The ZnO nanostructures fabricated with zinc acetate to PVA ratios of 2:3 and 1:1 exhibited approximately 31% and 28% IPCE, respectively, at about 350 nm compared with the ZnO nanostructures fabricated with zinc acetate to PVA ratios of 1:2 (7%) and 3:2 (4%) due to the increased number of nanostructures, resulting in the enhancement of light absorption and electron transfer rate.

Keywords

Zinc oxide, electrospinning, nanostructures, photoelectrochemical performance, zinc acetate, fiber precursor

Date received: 12 April 2016; accepted: 27 June 2016

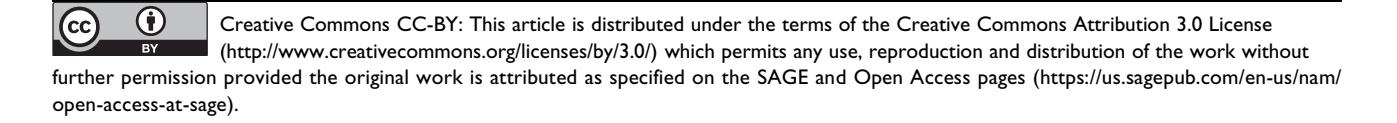
Topic: Nanophotonics Topic Editor: Marco Consales Associate Editor: Liam O'Faolain

Introduction

As an important *n*-type semiconductor with a bandgap energy of 3.37 eV and large exciton binding energy of 60 meV, ^{1,2} zinc oxide (ZnO) has received considerable attention because of its fascinating optical, magnetic, and piezoelectric properties. ³ ZnO has potential applications in dye-sensitized solar cell, gas sensors, and piezoelectric devices as an effective, low-cost, nontoxic, and suitable compound. ⁴⁻⁶ The one-dimensional nanostructures of ZnO can easily be synthesized in different forms. ⁷ such

Corresponding author:

Juan Rodriguez, Facultad de Ciencias, Universidad Nacional de Ingeniería, P.O. Box 31-139, Av. Túpac Amaru 210, Lima, Perú. Email: jrodriguez@uni.edu.pe



¹ Facultad de Ciencias, Universidad Nacional de Ingeniería, Lima, Perú

²Instituto de Química Física de los Materiales, Medio Ambiente y Energía (INQUIMAE), CONICET-UBA, Ciudad Universitaria, C1428EHA Buenos Aires, Argentina

³ Instituto de Investigación e Ingeniería Ambiental, Escuela de Ciencia y Tecnología, CONICET, Universidad Nacional de San Martín (UNSAM), Campus Miguelete, 25 de Mayo y Francia, 1650 San Martín, Provincia de Buenos Aires, Argentina

⁴Department of Natural and Mathematic Sciences, Turin Polytechnic University in Tashkent, Kichik Halqa Yo'li, Tashkent, Uzbekistan

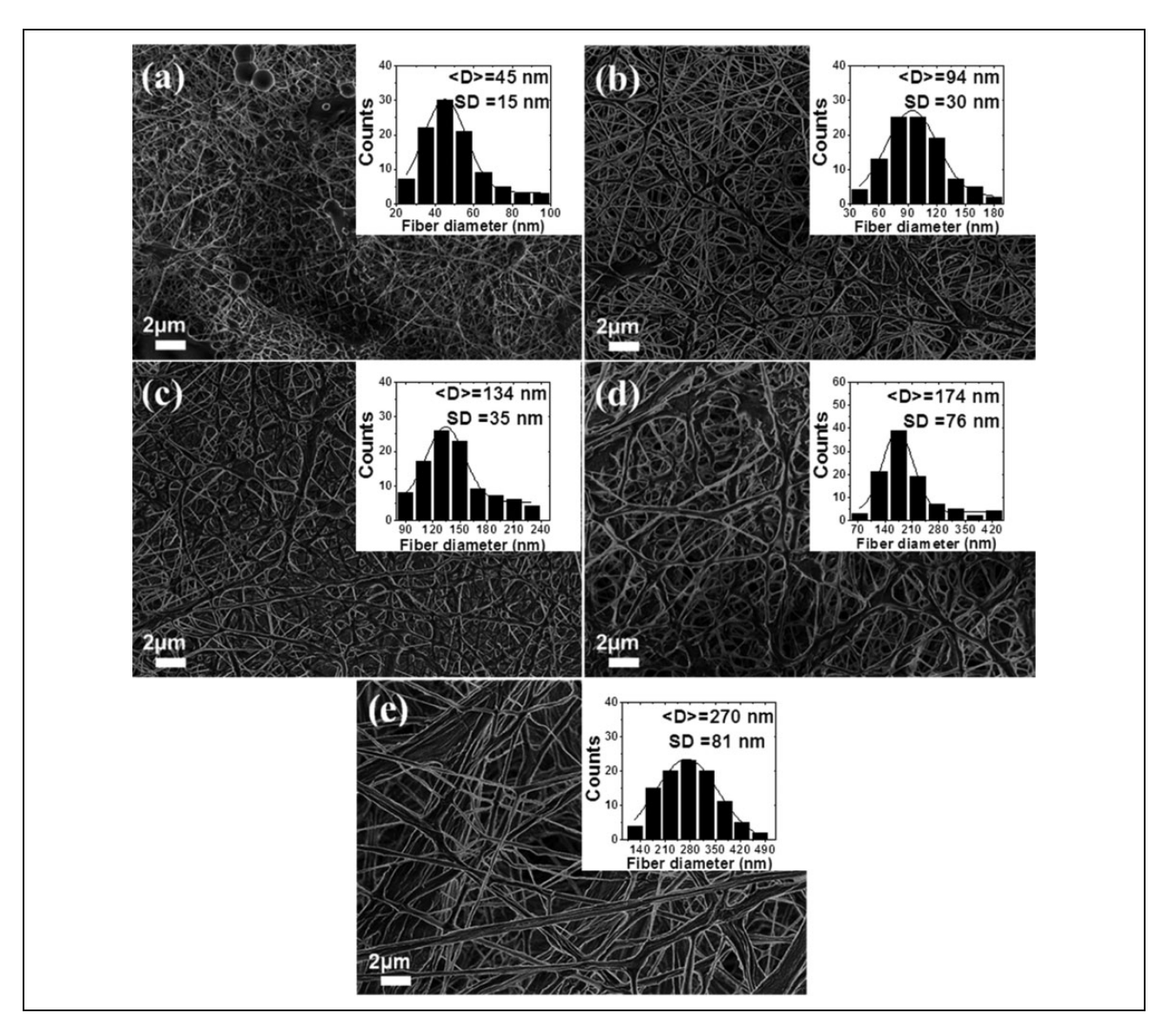


Figure 1. SEM images of precursor fibers prepared from the spinning solutions with different zinc acetate to PVA ratios: (a) PVA, (b) 1:2, (c) 2:3, (d) 1:1, and (e) 3:2. The diameter distributions of fibers with corresponding SD are shown as insets. SEM: scanning electron microscope; SD: standard deviation; PVA: polyvinyl alcohol.

as nanotubes, nanowires, nanorods, and nanofibers, and nanofibers, with different surface area to volume ratios and charge transfer efficiencies in comparison to spherical nanoparticles of ZnO, resulting in higher photocatalytic activity. 12 Particularly, the nanofibers possessing high surface area to volume ratio, extremely long length, and small diameter are considered to be suitable in solar cells, filtration, and biomedical applications. 13 Several techniques, including template synthesis, phase separation, self-assembly, and electrospinning, 14 have been applied to fabricate the nanofibers. Among them, electrospinning has been widely used to produce the nanofibers from polymeric precursor solution by applying an electrical potential between the end of an injection needle and a collector, where the nanofibers are deposited. 15 The electrospun nanofibers can double the surface area of the traditional thin films. 16 A number of

works have previously demonstrated the formation of ZnO nanofibers by applying electrospinning technique using the solution containing zinc acetate and various polymers, such as polyvinyl alcohol (PVA),¹⁷ polyvinylpyrrolidone,¹⁸ polyvinyl acetate, ¹⁹ or poly-acrylonitrile. ²⁰ However, the influence of zinc acetate content on the morphology, crystallinity, and photoelectrochemical performance of ZnO nanofibers was not reported in those studies. In this article, we therefore demonstrate the influence of zinc acetate content (zinc acetate to PVA mass ratio) on the morphology, crystallinity, and photoelectrochemical performance of ZnO nanostructures deposited on fluorine-doped tin oxide (FTO) glass substrate by electrospinning technique. The crystallinity, morphologies, and microstructures of ZnO nanostructures were analyzed by X-ray diffraction (XRD) and scanning electron microscopy (SEM), respectively.

Ramos et al. 3

The incident photon to current efficiency (IPCE) of the ZnO nanostructures was measured in a three-electrode cell, using a platinum wire as a counterelectrode and silver/silver chloride (Ag/AgCl) as a reference electrode.

Experimental

Fabrication

PVA ($M_W = 61,000$ g/mol; Sigma Aldrich, St Louis, USA) and zinc acetate dehydrate (Merck, New Jersey, USA) were used as the starting materials. The precursor nanofibers were fabricated in the following procedure: an agueous solution of PVA (14 wt%) was first prepared by dissolving 10 g of PVA powder in warm deionized water and then zinc acetate was slowly added into the PVA solution in different zinc acetate-to-PVA mass ratios (3:2, 1:1, 2:3, and 1:2). The spinning solution was homogenized by stirring at 60°C for 3 h. The electrospinning parameters were optimized after running a series of experiments. The obtained spinning solution was immediately transferred into a plastic syringe equipped with a blunt-ended 23-gauge stainless steel needle, which was connected to a high-voltage power supply. The electrical potential applied was 62 kV. The fabrication and deposition of the precursor nanofibers were conducted by a homemade electrospinning apparatus under ambient conditions using FTO glass as a rotating collector substrate placed 10 cm away from the tip of the needle. The feeding rate of the spinning solution (2 ml/h) was controlled with a syringe pump, and the deposition time was 2 h. In order to remove the polymer after the electrospinning process and to obtain ZnO nanostructures, the deposited precursor nanofibers were initially dried at 120°C for 6 h and then calcined at 600°C for 3 h.

Characterization

The XRD patterns of the calcined samples were recorded on a Philips X'PERT (Philips, The Netherlands) MPD (Multipurpose X-Ray Difracction System) with CuKα radiation ($\lambda = 1.5418 \text{ Å}$) in the 20 scan range of 20° to 80°. The morphologies and microstructures of the as-spun precursor nanofibers and ZnO nanostructures were observed using a Zeiss Supra 40 scanning electron microscope (Carl Zeiss, Germany) equipped with an energy dispersive X-ray spectroscopy. The viscosity measurements were made using 25 g of mixture into a Brookfield DV III-ULTRA rheometer (Brookfield, USA). The IPCE spectra of the ZnO nanostructures obtained by calcination of the as-spun precursor nanofibers were measured using a potentiostat/galvanostat (PG580; Uniscan Instruments, USA) in a three-electrode cell, using the fabricated ZnO nanostructures as a working electrode, a platinum wire as a counterelectrode, Ag/AgCl electrode immersed in 0.1 M KCl solution as a reference electrode, 0.1 N NaOH as an

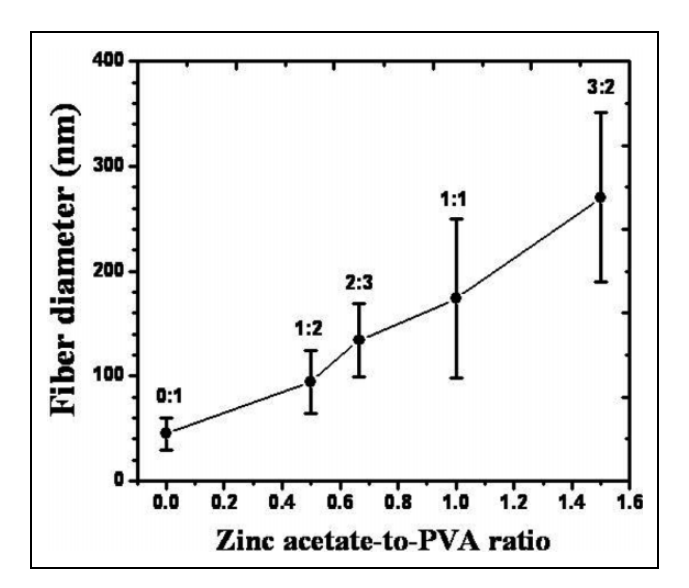


Figure 2. Diameters of precursor fibers as a function of zinc acetate to PVA ratio. The error bars represent a standard deviation of the fiber diameter. SD: standard deviation; PVA: polyvinyl alcohol.

electrolytic solution, and a 400–1000 W Xe lamp coupled with an Oriel Cornerstone 130 monochromator (Oriel Instruments, USA) as a light source. The light intensity was in the range of 0.10–2.10 mW/cm².

Results and discussion

Figure 1 shows the SEM images of the as-spun precursors fibers obtained by electrospinning technique. As shown, the precursor fibers have a smooth surface without beads in contrast to the precursor fibers formed from only PVA because of low viscosity and high voltage applied.²¹ The XRD results (not shown here) revealed that ZnO is not in the crystalline form in the precursor fibers. By increasing the amount of zinc acetate loaded in the spinning solution, the diameters of the precursor fibers enlarged from 45 to 270 nm. It should be noted that as the amount of zinc acetate increased, not only was there an increase in the diameter of the precursor but also the distribution became broader (Figure 2). This is a result of the increase in the viscosity of the spinning solution by increasing the amount of zinc acetate because of the gelation of zinc acetate (621 cP for PVA<658 cP for 1:2<690 cP for 2:3 < 722 cP for 1:1 < 752 cP for 3:2). The increased viscosity can lead to non-uniform ejection of the jet,²² and it is hence responsible for the broad diametric distribution of the precursor fibers prepared from the spinning solution containing high amount of zinc acetate.

The SEM images of ZnO nanostructures obtained by calcination of the precursor fibers at 600°C are shown in Figure 3. It is evidenced that the diameters of ZnO nanostructures became smaller compared to that of precursor fibers due to the decomposition of PVA and the crystallization of ZnO during calcination. It is clear that even

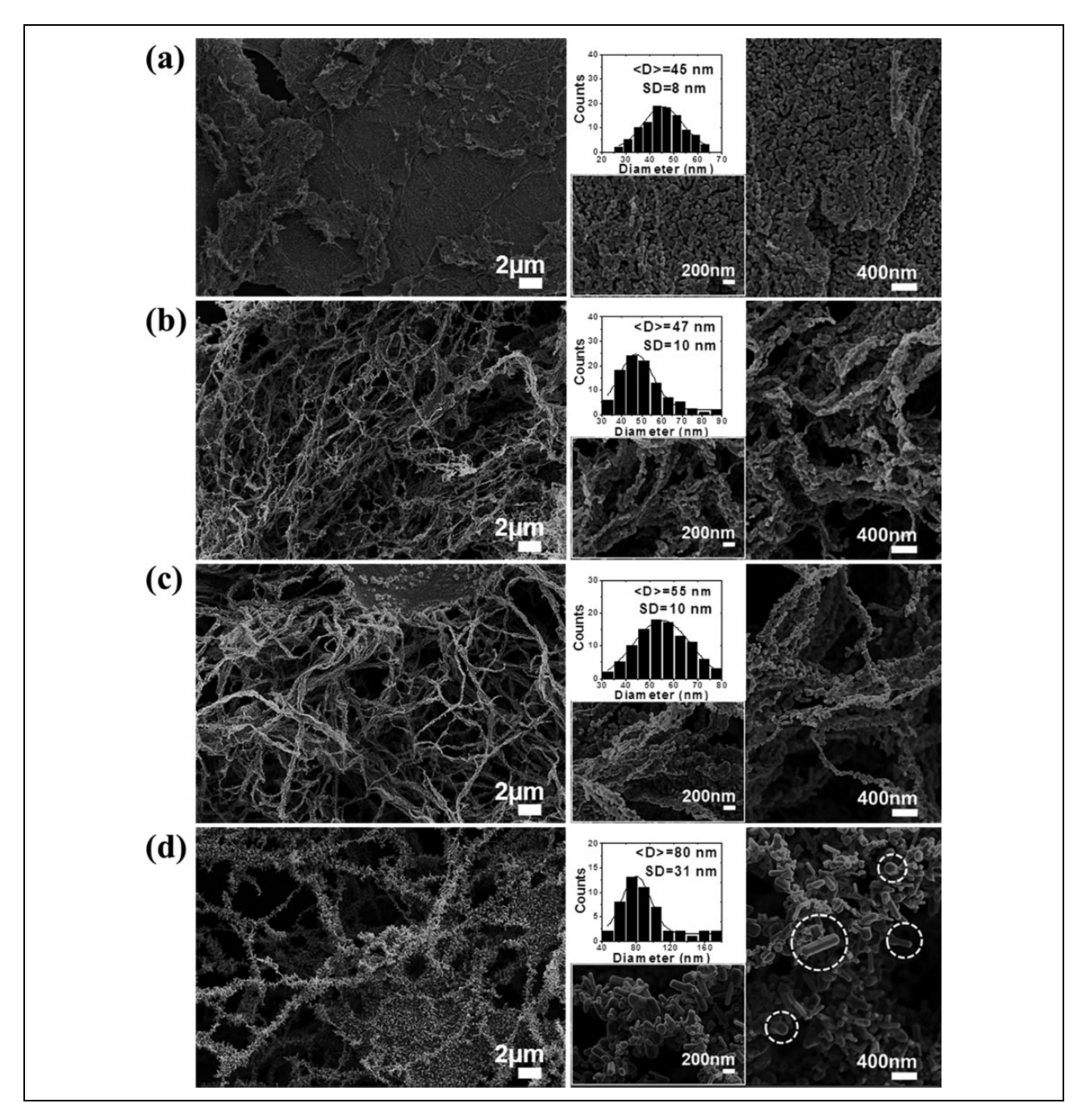


Figure 3. SEM images of ZnO nanostructures obtained by calcination of precursor fibers prepared from the spinning solutions with different zinc acetate to PVA ratios: (a) 1:2, (b) 2:3, (c) 1:1, and (d) 3:2. The diameter distributions of ZnO nanocrystals with a SD and high-magnification SEM images are shown as insets. SD: standard deviation; PVA: polyvinyl alcohol; SEM: scanning electron microscopy; ZnO: zinc oxide.

though the PVA was completely decomposed, the nanostructures of ZnO are governed by the amount of zinc acetate in the spinning solution. The mean diameters of the nanoparticles forming the ZnO nanostructures increased with increasing the amount of zinc acetate in the following order: 45 nm for 1:2 <47 nm for 2:3 <55 nm for 1:1 <80 nm for 3:2. The results suggest that the dispersed zinc acetate clusters in the PVA matrix of the precursor fibers can act as

nucleation sites upon calcination,²³ resulting in the growth of ZnO nanocrystals on the electrospun fibers. According to the literature,²⁴ the ZnO nanostructures can also be obtained with lower concentration (1:2) because the ZnO nuclei are well separated and unable to form primary particles during the calcination process resulting in nanofibers with a large area of ordered atomic arrangement (Figure 3(a)). In contrast, higher precursor concentrations

Ramos et al. 5

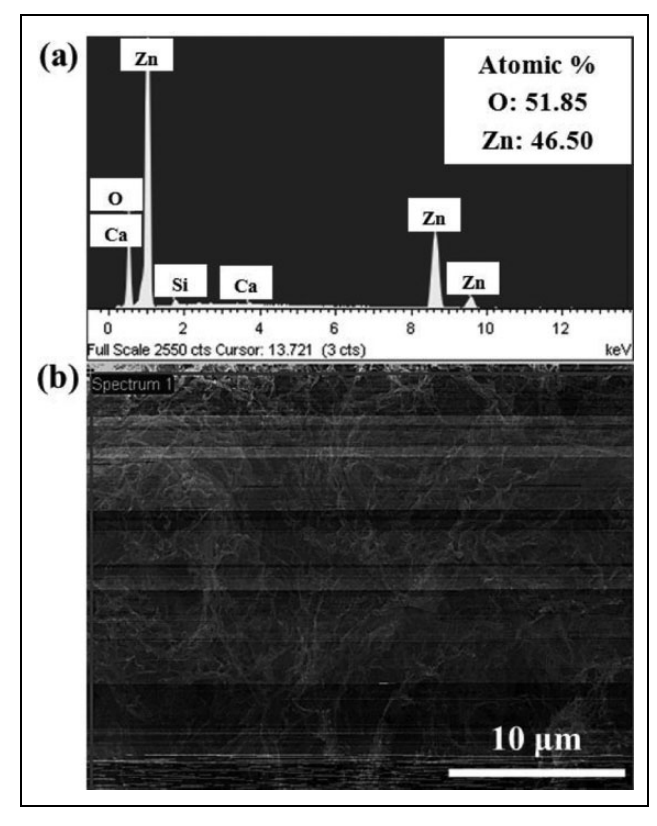


Figure 4. (a) Energy-dispersive X-ray spectroscopy (EDS) spectrum and (b) SEM image of ZnO nanostructures obtained by calcination of precursor fibers prepared from the spinning solution with zinc acetate to PVA ratio of 2:3. PVA: polyvinyl alcohol; SEM: scanning electron microscopy; ZnO: zinc oxide.

lead to nanofibers with larger nanoparticles connected along the fiber axis. This is due to the formation of primary particles during the calcination process prior to the complete decomposition of the polymer matrix (Figure 3(d)). Further, Figure 3(d) shows the SEM images of the ZnO nanostructures obtained by calcination of precursor fibers prepared from the spinning solution with zinc acetate to PVA ratio of 3:2. As shown, the crystals with an average diameter of 73 nm and nanorods with an average diameter of 80 nm and a length in the range of 300–500 nm were formed. The formation of nanorods along with small particles of ZnO with undefined shapes was a result of oriented attachment growth.²⁵

The Energy-dispersive X-ray spectroscopy (EDS) spectrum of the ZnO nanostructures showed in Figure 4 confirms the complete decomposition of the PVA and the crystallization of ZnO after calcination of precursor fibers. The peaks associated with zinc and oxygen can be seen in the EDS spectrum, while the peak associated with carbon is not observed, evidencing the successful conversion of precursor fibers into ZnO nanostructures.

The XRD patterns of ZnO nanostructures obtained by calcination of the precursor fibers at 600°C are shown in Figure 5(a). Compared to the XRD pattern of substrate, the XRD patterns of nanostructures contain six main

diffraction peaks corresponding to the (100), (002), (101), (102), (110), and (103) crystallographic planes of hexagonal wurtzite structure of ZnO (ICDD PDF# 36-1451). The (101) plane indicates the preferential growth of the ZnO nanostructures with wurtzite structure fabricated by electrospinning. It is evident that the intensity of the (101) diffraction peak of ZnO nanostructures gradually increased with increased amount of zinc acetate because a large number of ZnO nanocrystals were formed. However, the ZnO nanostructures fabricated with zinc acetate to PVA mass ratio of 3:2 showed a diffraction peak corresponding to the crystallographic plane of (002) with intensity closer to that of the diffraction peak corresponding to the crystallographic plane of (101). This implies that some crystals have an oriented growth in this direction (002), and similar phenomenon was previously observed for ZnO nanorods. 26,27 The diffraction peaks represent the typical widths of nanocrystalline materials. The mean size of the crystalline domain was estimated for each sample from the full width at a half maximum (FWHM) of the (101) peak using the Scherrer's equation: $D = 0.9 \lambda / \beta \cos(\theta)$, where λ is the X-ray wavelength of the Cu K α radiation (1.5418 Å), θ is the diffraction angle, and β is the FWHM of the diffraction peak. For all samples, D lies in the range of 28-32 nm, which gradually increases with increasing the amount of

The IPCE spectra are plotted in Figure 5(b) as a function of wavelength. As shown, the ZnO nanostructures fabricated with zinc acetate to PVA mass ratio of 2:3 showed the highest IPCE value in the wavelength range from 330 to 420 nm compared with other ZnO nanostructures fabricated with zinc acetate to PVA mass ratios of 1:2, 1:1, and 3:2. Although the ZnO nanostructures fabricated with zinc acetate to PVA mass ratio of 3:2 contained the highest amount of zinc acetate, they showed the lowest IPCE value in the wavelength range from 330 to 420 nm. Depending on zinc acetate to PVA mass ratio, the IPCE value of the ZnO nanostructures increases in the following order: 4% for 3:2 <7% for 1:2 <28% for 1:1 <31% for 2:3 at about 350 nm. The main difference in the IPCE values of the ZnO nanostructures is presumably attributed to the enhanced light absorption, electron transfer rate, and delayed charge recombination, ²⁸⁻³⁰ which depend on the morphology, adhesion to the substrates,³¹ and specific surface area of the ZnO nanostructures.³² In the case of the ZnO nanostructures fabricated with zinc acetate to PVA mass ratios of 3:2, 1:1, and 2:3, the number of nanofibers increased as the amount of zinc acetate in the spinning solution decreased, covering the surface of FTO glass (Figure 5(c)). It is thought that the reason for the highest efficiency of the ZnO nanostructures fabricated with zinc acetate to PVA mass ratio of 2:3 is good adhesion, the presence of a number of nanofibers (Figure 5(c)), and the small crystal size (Figure 3(c)), resulting in large surface area and enhanced light absorption.²⁹ Unlike the ZnO nanostructures fabricated with zinc acetate to PVA mass ratio of 3:2 having

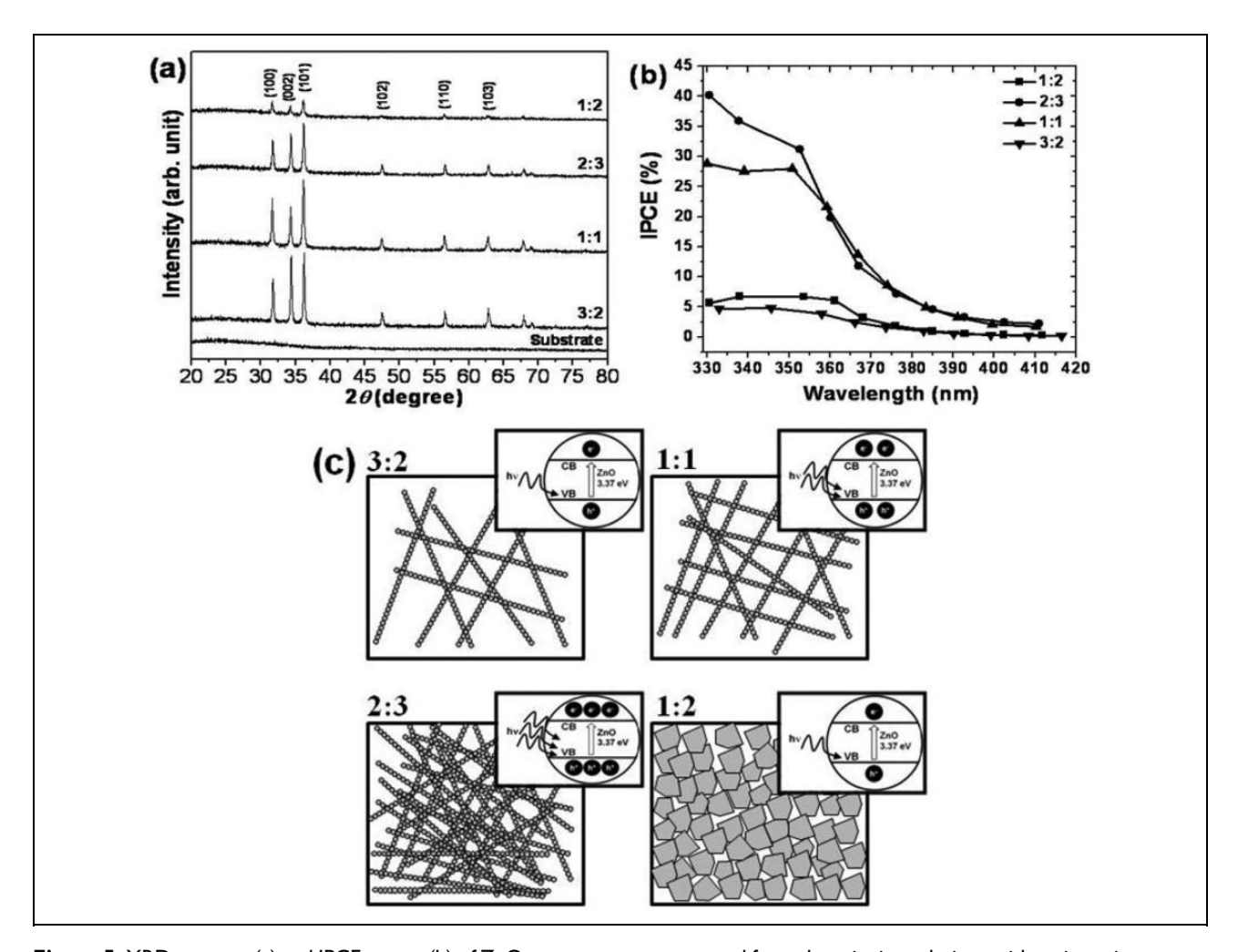


Figure 5. XRD patterns (a) and IPCE curves (b) of ZnO nanostructures prepared from the spinning solutions with various zinc acetate to PVA ratio: I:2, 2:3, I:1, and 3:2. (c) Schematic illustration of the influence of zinc acetate to PVA ratio on morphology, light absorption, and electron transfer rate of the ZnO nanostructures fabricated in this study. XRD: X-ray diffraction; IPCE: incident photon to current efficiency; ZnO: zinc oxide; PVA: polyvinyl alcohol.

the lowest efficiency due to large crystal size (Figure 3(d)) and the presence of a few nanofibers (Figure 5(c)), resulting in a low electron transfer rate and low light absorption.²⁹ Despite the fact that the ZnO nanostructures fabricated with zinc acetate to PVA mass ratio of 1:2 fully covered the surface of FTO glass in the form of thick film, they exhibited a low IPCE value possibly due to the existence of grain boundaries and voids in the nanostructures, hindering an efficient transfer of photogenerated electrons.³¹ The results of this study showed that the zinc acetate to PVA mass ratio was critical and must be controlled in order to enhance the electron transfer rate, to increase the efficiency of capturing the light, and to achieve the highest IPCE value.

Conclusions

In summary, the influence of zinc acetate to PVA mass ratio on the morphology, crystallinity, and photoelectrochemical performance of ZnO nanostructures obtained by calcination at 600°C for 3 h of precursor fibers prepared

from the spinning solution with zinc acetate to PVA ratios of 1:2, 2:3, 1:1, and 3:2 was investigated. The mean diameter of the ZnO nanoparticles forming the nanostructures ranged from 45 to 80 nm with increasing the amount of zinc acetate. The ZnO nanostructures fabricated with zinc acetate to PVA ratios of 2:3 and 1:1 exhibited approximately 31% and 28% IPCE, respectively, at about 350 nm compared with the ZnO nanostructures fabricated with zinc acetate to PVA ratios of 1:2 (7%) and 3:2 (4%) due to the increased number of nanostructures, resulting in enhancement of light absorption and electron transfer rate.

Declaration of conflicting interests

The author(s) declared no potential conflicts of interest with respect to the research, authorship, and/or publication of this article.

Funding

The author(s) disclosed receipt of the following financial support for the research, authorship, and/or publication of this article: Ramos et al. 7

The present work was supported by the FINCyT Project (no. 140-FINCYT-IB-2013) and FONDECYT Project (No 223, CONCY-TEC-2015). PGR would like to thank the Peruvian Council for Science and Technology (CONCYTEC) for the Scholarship. The authors are grateful to Dr. Claudia Marchi and Dr. Luis Sanchez for their excellent technical assistance in SEM observation and XRD analysis. MH would also like to thank the World Academy of Sciences (TWAS) for Visiting Expert Programme (F.R. 32402182000).

References

- Chen X, Zhai Y, Li J, et al. Increased photocatalytic activity of tube-brush-like ZnO nanostructures fabricated by using PVP nanofibers as templates. *Appl Surf Sci* 2014: 319: 216–220.
- 2. Yu H, Fan H, Wang X, et al. Synthesis and optical properties of Co-doped ZnO nanofibers prepared by electrospinning. *Optik–Int J Light Elect Optics* 2014; 125: 2361–2364.
- 3. Kanjwal MA, Sheikh FA, Barakat NAM, et al, Co₃O₄–ZnO hierarchical nanostructures by electrospinning and hydrothermal methods. *Appl Surf Sci* 2011; 257: 7975–7981.
- Li F, Wang G, Jiao Y, et al. Efficiency enhancement of ZnO-based dye-sensitized solar cell by hollow TiO₂ nanofibers. *J Alloys Compd* 2014; 611: 19–23.
- Wei S, Wang S, Zhang Y, et al. Different morphologies of ZnO and their ethanol sensing property. Sensor Actuators B Chem 2014; 192: 480–487.
- 6. Park JY, Kim J-J, and Kim SS. Electrical transport properties of ZnO nanofibers. *Microelect Eng* 2013; 101: 8–11.
- Wang ZL. Nanostructures of zinc oxide. *Mater Today* 2004;
 26–33.
- Luo L, Lv G, Li B, et al. Formation of aligned ZnO nanotube arrays by chemical etching and coupling with CdSe for photovoltaic application. *Thin Solid Films* 2010; 518: 5146–5152.
- Elias J, Tena-Zaera R, and Lévy-Clément C. Electrochemical deposition of ZnO nanowire arrays with tailored dimensions. *J Electroanal Chem* 2008; 621: 171–177.
- Sanchez L, Guz L, García P, et al. Synthesis and characterization of ZnO nanorods films on PET for photocatalytic disinfection of water. *J Adv Oxid Technol* 2015; 18: 246–252.
- 11. Park J-A, Moon J, Lee S-J, et al. Fabrication and characterization of ZnO nanofibers by electrospinning. *Curr Appl Phys* 2009; 9: S210–S212.
- 12. Lee HU, Park SY, Lee SC, et al. Highly photocatalytic performance of flexible 3 dimensional (3D) ZnO nanocomposite. *Appl Catal B* 2014; 144: 83–89.
- 13. Panthi G, Park M, Kim H-Y, et al. Electrospun polymeric nanofibers encapsulated with nanostructured materials and their applications: a review. *J Ind Eng Chem* 2015; 24: 1–13.
- 14. Ramakrishna S, Fujihara K, Teo W-E, et al. *An introduction to electrospinning and nanofibers*. Singapore: World Scientific Publishing, 2005.
- 15. Merritt SR, Exner AA, Lee Z, et al. Electrospinning and imaging. *Adv Eng Mater* 2012; 14: B266–B278.

 Jin L, Wang T, Zhu M-L, et al. Electrospun fibers and tissue engineering. J Biomed Nanotechnol 2012; 8: 1–9.

- Samadi M, Pourjavadi A and Moshfegh AZ. Role of CdO addition on the growth and photocatalytic activity of electrospun ZnO nanofibers: UV vs. visible light. *Appl Surf Sci* 2014; 298: 147–154.
- Ren P, Fan H, and Wang X. Electrospun nanofibers of ZnO/BaTiO₃ heterostructures with enhanced photocatalytic activity. *Catal Commun* 2012; 25: 32–35.
- Murugan R, Babu VJ, Khin MM, et al. Synthesis and photocatalytic applications of flower shaped electrospun ZnO– TiO₂ mesostructures. *Mater Lett* 2013; 97: 47–51.
- Singh P, Mondal K, and Sharma A. Reusable electrospun mesoporous ZnO nanofiber mats for photocatalytic degradation of polycyclic aromatic hydrocarbon dyes in wastewater. *J Colloid Interface Sci* 2013; 394: 208–215.
- Zhenyu L and Wang C. One-dimensional Nanostructures: electrospinning technique and Unique Nanofibers. Berlin: Springer, 2013.
- 22. Yang R-R, He J-H, Xu L, et al. Effect of solution concentration on diameter and morphology of PVA nanofibers in bubble electrospinning process. *Mater Sci Tech Ser* 2010; 26: 1313–1316.
- Sangkhaprom N, Supaphol P, and Pavarajarn V. Fibrous zinc oxide prepared by combined electrospinning and solvothermal techniques. *Ceram Int* 2010; 36: 357–363.
- Muangban J and Jaroenapibal P. Effects of precursor concentration on crystalline morphologies and particle sizes of electrospun WO₃ nanofibers. *Ceram Int* 2014; 40: 6759–6764.
- Archana J, Navaneethan M, and Hayakawa Y. Morphological transformation of ZnO nanoparticle to nanorods via solid– solid interaction at high temperature annealing and functional properties. *Scr Mater* 2016; 113: 163–166.
- Li Y, Gong J, and Deng Y. Hierarchical structured ZnO nanorods on ZnO nanofibers and their photoresponse to UV and visible lights. Sensor Actuat A Phys 2010; 158: 176–182.
- Dong X, Yang P, and Shi R. Fabrication of ZnO nanorod arrays via electrospinning assisted hydrothermal method. *Mater Lett* 2014; 135: 96–98.
- Wijeratne K and Bandara J. Aspect-ratio dependent electron transport and recombination in dye-sensitized solar cells fabricated with one-dimensional ZnO nanostructures. *Electrochim Acta* 2014; 148: 302–309.
- Fang J, Fan H, Tian H, et al. Morphology control of ZnO nanostructures for high efficient dye-sensitized solar cells. *Mater Char* 2015; 108: 51–57.
- Ganesh T, Bhande SS, Mane RS, et al. Crystallographic phase-mediated dye-sensitized solar cell performance of ZnO nanostructures. Scr Mater 2013; 69: 291–294.
- Thavasi V, Renugopalakrishnan V, Jose R, et al. Controlled electron injection and transport at materials interfaces in dye sensitized solar cells. *Mater Sci Eng R-Rep* 2009; 63: 81–99.
- 32. Dong X, Yang P, Liu Y, et al. Morphology evolution of onedimensional ZnO nanostructures towards enhanced photocatalysis performance. *Ceram Int* 2016; 42: 518–526.